Article ID: 1003 - 6326(2003)05 - 1194 - 05

Pore opening and binder flow during initial stage of thermal debinding in MIM①

ZHAO Li-gang(赵利刚)[1], LI Yi-min(李益民)[1, 2]
(1. State Key Laboratory for Powder Metallurgy, Central South University, Changsha 410083, China;
2. Hunan Injection Hi-Tech Ltd Changsha 410083, China)

Abstract: Pore opening and binder flow during the initial stage of thermal debinding in metal injection molded parts was investigated. Scaning electron microscopy(SEM) pictures of 316 L stainless steel parts using wax-based binder show that small particles will move to the surface with the process of debinding. SEM pictures of different mass loss rate specimens indicate that initial pores will emerge when as little as 4% binder removes. During the initial stage of thermal debinding, vapor tension varies in different place due to the difference of curvature. Thus more binders will be removed in places with smaller cavity between metal powders, and in these places small openings emerge.

Key words: metal injection molding; thermal debinding; pore opening; binder flow
CLC number: TF 125.3 **Document code:** A

1 INTRODUCTION

Metal injection molding(MIM) is a net-shaping technology, which has the characteristics of the plastic injection molding and conventional powder metallurgy(PM). MIM enables the production of products with greater shape complexity, and with better performances. This process consists of the following steps: certain amount of binder is blended with proper powders, in order for preparing suitable feed-stocks to injection; after injection molding, parts are debound and then sintered and in this way final products are formed[1, 2].

The debinding process has been considered to be the most critical step in MIM because of the long time needed to burn out the binders without introducing defects, such as blistering, warping, and skin exfoliation[3]. Although these defects can be caused by some related factors, such as non-uniform green density, poor mold design and heterogeneously mixed feedstock, the major challenge comes from the debinding process itself. Basic debinding mechanism includes thermal debinding, solvent debinding, wick debinding, etc[4]. Thermal debinding is of great popularity, especially when wax-based binder is used.

The process of thermal debinding can be divided into three steps: initial stage, intermediate stage, and final stage[3]. It's commonly assumed that connected pores will be formed in the MIM parts after about 40% (volume fraction) binders have been removed, then the debinding cycle enters into the intermediate stage. The stage before connected pores formed can be defined as initial stage.

Considerable efforts have been made to understand the process and mechanism of thermal debinding. There are many reports concerning the research of thermal debinding, but most of them are about the middle and the final stage[5-8], few are concentrating on the initial stage[9]. Among the few researches on the initial stage, some hypotheses have been made to explain the debinding process. But these hypotheses haven't been confirmed experimentally.

German[10] modeled isothermal debinding by two separate controlling mechanisms: vapor diffusion and vapor permeation. He described the movement of the binder liquid front and studied the parameters which could affect the stability of the binder fluid. He suggest that the binder decompose at the binder/gas interface, and the evolving gas diffuse or permeate to the surface through the inter-particle voids. As debinding continues, the binder front progressively retreats toward the center of the body.

Hwang et al[11] made the conclusion that during the initial stage of debinding, small openings would emerge in the surface of the samples. But as to how these openings evolved, no explanation was given.

In this paper, the initial stage of thermal debinding is studied and the debinding mechanism for a mul-

① **Foundation item:** Project(50044012) supported by the National Natural Science Foundation of China; project(2001AA337050) supported by the National Advanced Materials Committee of China; project(200135) supported by the Special Funds for National Excellent PhD Thesis Authors of China and project(81041) supported by HUO Yin-dong Education Foundation
Received date: 2002 - 11 - 11; **Accepted date:** 2003 - 03 - 06
Correspondence: LI Yi-min, Professor; Tel: + 86-731-8836113; E-mail: rockyzhao@163.com

tri-component binder system is investigated. SEM is applied to observe the pore structure and binder distribution.

2 EXPERIMENTAL

Present MIM industry mainly focuses on stainless steel, among others 316 L stainless steel accounts for 50%[12]. The interaction between binder and powder greatly depends on the shape of powders(except for reactive materials). Gas atomized 316 L stainless steel powder(produced by Osprey Company, England) is spherical. This shape is close to the ideal shape of MIM powders[13]. So, gas atomized 316 L stainless steel powder was used in this study. The characteristics of this powder are listed in Table 1.

A multi-component binder system was used to prepare the feedstock. The binder consisting of paraffin wax(PW), ethylene vinyl acetate(EVA), high-density polyethylene(HDPE) and stearic acid(SA), was believed to have good rheology characteristics and fluidity[9]. The melting temperature of each component is listed in Table 2.

Gas atomized powders were first dryly blended with PW-EVA-HDPE-SA binder in a YHL01 blender for 45 min. The blended powder was then mixed by an XSM1/20-80 plastics blender at 150 ℃ for 2 h, and followed by extrusion in a two-screw extruder for three times to get a more uniform mixture suitable for injection molding. The mixture was cooled to room temperature, then granulated into 1~5 mm particles by a granulator, which serves as a feedstock. Powder loading of this feedstock was 64%.

Disc-shaped parts with a diameter of 20 mm and thickness of 4 mm were made by BOY50T2 injection-molding machine. The molding pressure was 110 MPa. The nozzle temperature was kept at 115 ℃ while the mold temperature was kept at 60 ℃ and the holding time was 4.5 s. Molded samples were thermally debound under hydrogen protection in a thermal debinding stove and debinding temperature was 150 ℃ and 165 ℃, respectively.

For direct observation of surface structure(external and fracture surface), a JSM-5600LV scanning electron microscope was used. SEM samples were sprayed with very fine gold powders for electric conduction. SEM pictures of different mass loss samples were taken to find out when small opening emerges. Here, mass loss percentage was determined as the ratio of mass loss against total binder mass in the sample.

3 RESULTS AND DISCUSSION

3.1 Mass loss analysis during initial stage of thermal debinding

According to the properties of binder components mentioned above, at 165 ℃ only paraffin wax begins to be debound.

Fig. 1 shows the relationship between mass loss percentage and debinding time at 150 ℃ and 165 ℃, respectively. It can be seen that accumulative mass loss at 150 ℃ increases very slowly while holding time prolongs, and when the mass loss reaches 2%, the debinding curve becomes flat, which means that debinding finishes at this temperature. Debinding mass loss evolving tendency at 165 ℃ is similar to that at 150 ℃, but the curve tends to become flat much quickly, and the mass loss at 165 ℃ is much higher than that at 150 ℃, which reaches 4%.

SEM photographs of different mass loss samples show that only in those samples with a mass loss larger than 4% can initial openings be observed. In samples debound at 150 ℃ no distinct openings are observed, while in those debound at 165 ℃ initial openings is watched clearly, as shown in Figs. 2 and 3. Fig. 2 shows SEM fractograph of debound parts (mass loss 4.4%, debinding temperature 165 ℃, holding time 480 min). Fig. 3 shows the schematic of Fig. 2. In the two photographs very small pores in the surface of debound parts can be seen, and these pores stretch into the center of the parts. This phenomenon can be explained as follows: in thermal debinding furnace, binder will melt into liquid phase, which is easy to move, then liquid binders fill the pores between powder particles. According to the theory of capillary flowing, capillary force generated by the liquid binders can suck internal binders out.

3.2 Forming mechanism of initial openings in surface

At low temperature, inter-space between powderparticles is filled with binders. With increasing

Table 1 Properties of gas atomized 316 L stainless steel powder

Powders	Chemical component/%					Fisher granularity/ μm	Tap density/ ($g \cdot cm^{-3}$)	Theoretical density/ ($g \cdot cm^{-3}$)
	C	Cr	Ni	Mo	Fe			
316 L SS	≤0.03	17	14	2	Balance	22	3.8	8

Table 2 Density and melting temperature of binder components

Component	t_m/ ℃	ρ/ (g·cm^{-3})
PW(paraffin wax)	58	0.91
EVA(ethylene-vinyl acetate)	80	0.96
HDPE(high-density poly-ethylene)	139	0.98
SA(stearic acid)	66	0.96

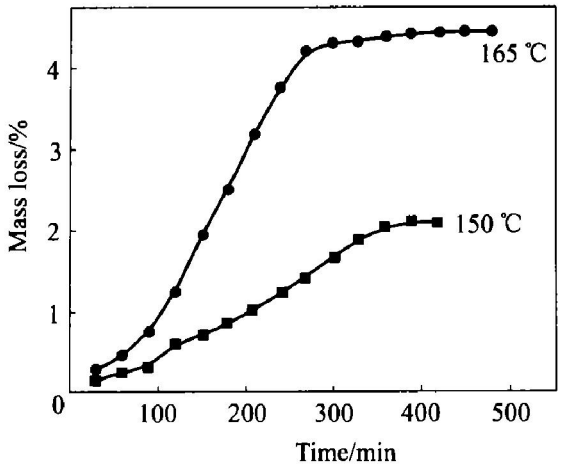

Fig. 1 Schematic of debinding curve under different temperature

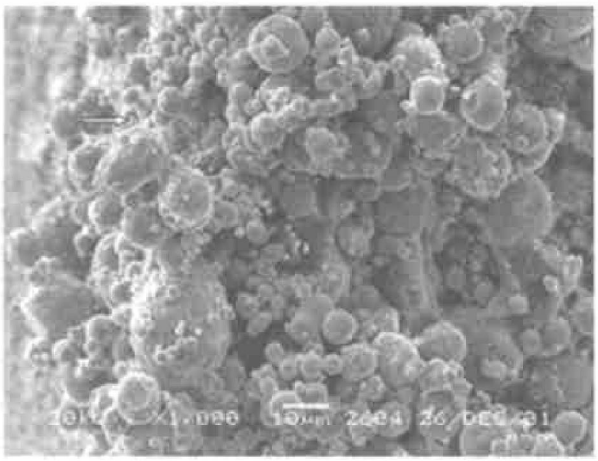

Fig. 2 Forming of initial opening

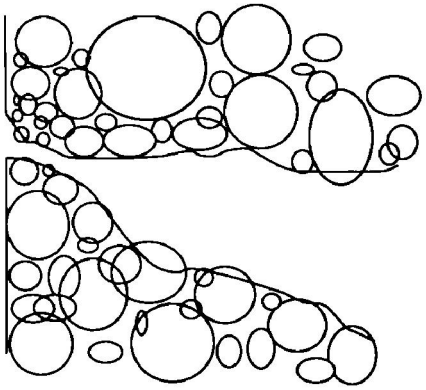

Fig. 3 Schematic of Fig. 2

temperature, binders begin to melt. When it reaches a certain temperature, every component melts, and paraffin wax begins to vaporize. Because of the present of many small metal powder particles, the surface of injection-molded parts is microcosmically not a plane. And because of the uneven particle size, there will be many unequally-sized pores between particles, where binders inhabit. These melted binders will serve as the liquid in a capillary tube, according to Kalwen equation

$$Rt \ln \frac{p'}{p^0} = \frac{2\gamma M}{\rho r}$$

where R is universal gas constant, 8.314 J/(K^{-1}·mol^{-1}); t is temperature, ℃; p' is polymer vapor pressure in pores, Pa; p^0 is polymer vapor pressure in plane, Pa; γ is liquid surface tension, N·m^{-1}; M is mole mass of liquid, kg·mol^{-1}; ρ is density of liquid, kg·m^{-3}; r is radius of pore, m; at certain temperature, γ, M, ρ, R, T and p^0 are all constants.

If binders form concave liquid exterior in places between metal particles, 'r' will be negative. Thus based on the above equation, binder vapor pressure in smaller inter-space will be smaller than that in larger inter-space. So vapor pressure in smaller inter-space will be saturated earlier than that in larger inter-space, and then this binder will condense to become liquid again, as a result the liquid exterior in smaller inter-space will be protruding, in this way, 'r' becomes positive. Here the above Kalwen equation was used again, as the pore radius is smaller in smaller inter-space, the vapor pressure will be larger, so the polymer binders will be preferentially removed in these places.

Or else, if binders form protruding liquid exterior in places between metal particles, 'r' will be positive. In this circumstance, according to the Kalwen equation, as the pore radius is smaller in smaller inter-space, the vapor pressure will be larger, so the polymer binders will be preferentially removed in these places. This discussion is in accordance with that of the above paragraphs.

With the constant removing of binders, there will be real pores in small inter-space between metal particles. This is the forming mechanism of small openings during thermal debinding.

Fig. 4 shows the SEM image of debound parts' external surface, the debinding temperature is 165 ℃, the holding time is 150 min, and the mass loss is 1.93%. Fig. 5 shows its schematic. Figs. 4 and 5 show that binders locating between small particles have been removed completely, while most of those locating between large metal powder particles remain. This is consistent with the discussion on vapor pressure mentioned above.

3.3 Binder flow and particle rearrangement

After the generating of small openings in the parts' surface, melted binder inside the parts will be dragged out by capillary force. Along binders flowing from inside to the exterior, small metal powder parti-

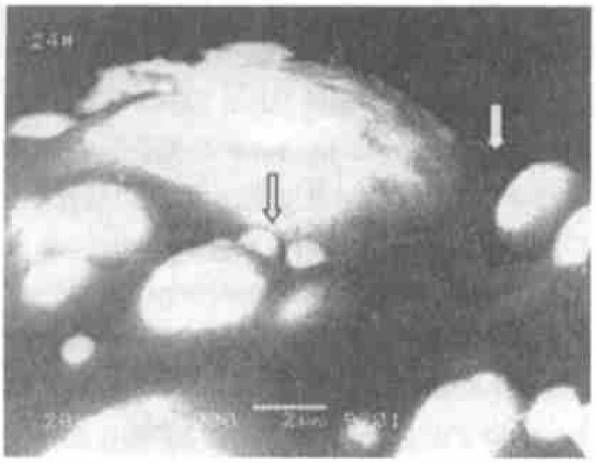

Fig. 4 SEM image of external surface (at 165 ℃ for 150 min)

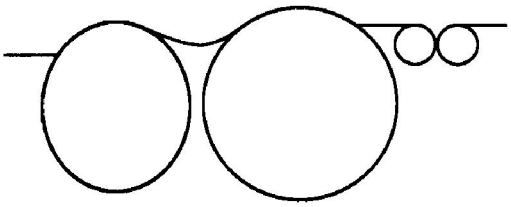

Fig. 5 Schematics of Fig. 4

cles inside the parts will also flow to the surface, thus the diameter of the small openings will be much smaller. The expression for capillary force can be written as

$$p_s = \frac{2\gamma}{r}$$

where p_s is extra pressure subjected by capillary tube, Pa; γ is liquid surface tension, $N \cdot m^{-1}$; r is radius of inter-space, m.

Based on the above formula, when liquid binders locate between the powder particles, attraction force in smaller inter-space will be larger. So binders in larger inter-space will be dragged to these places. Also based on the above discussion on the forming mechanism of surface openings, very fine openings will emerge in the parts' surface and because of the capillary force, internal binders will flow to the surface. Therefore, in this way initial openings form. At the same time, small metal powder particles inside the parts will also flow with the binders. Figs. 6 and 7 show SEM micrographs of green parts and of light debinding (debinding temperature 165 ℃, holding time 270 min, mass loss 4.2%). Statistically, the ratio of small powder particles' amount ($\leqslant 5$ μm) to the big ones' (> 5 μm) in the green parts surface is 4.8, while this data of debound parts become 5.9. This phenomenon can be explained as follows: because of binder flowage during debinding, smaller powder particles will be forced to move to the part's surface

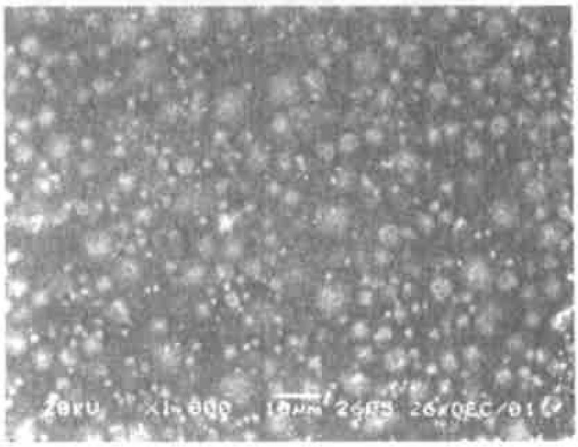

Fig. 6 SEM micrograph of green parts

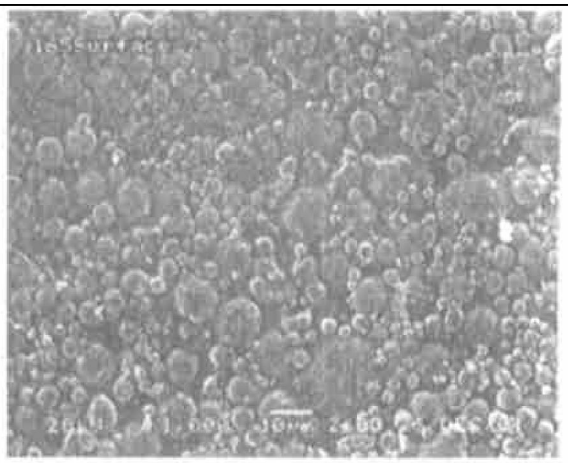

Fig. 7 SEM micrograph of debound parts' surface

along with the binders, as a result smaller powder particles will be much more on the surface. The smaller the powder particle's diameter, the larger its surface energy is. This means that the parts can be sintered at a lower temperature. The flowage tendency of smaller metal powder particles is very preferential to the MIM part's densification during sintering[14].

As to the debinding performance after the forming of initial pores, there have been already many reports, and their conclusions fit experiments very well. At present, a broadly accepted theory is[15, 16]: after the forming of initial pores, these pores' internal surfaces will serve as part's surface and new pores will emerge in these places, finally, great amount of connected pores will be formed. Through these connected pores binders will be removed continuously and debinding will be very quick in this stage.

4 CONCLUSIONS

1) Only after 4% binders have been removed initial pores can emerge when PW-EVA-HDPE-SA binder system is used.

2) In the initial stage of thermal debinding, due

to the difference of polymer vapor pressure in places with different curvature radius, binders between small powder particles will be removed much more quickly, while debinding of those between bigger powder particles will be comparatively slower.

3) During thermal debinding, metal powder particle's position will be rearranged because of capillary force. Some of the smaller powder particles will move to the surface.

REFERENCES

[1] German R M, Hens K F, Lin S P. Key issues in powder injection molding[J]. Ceramic Bulletin, 1991, 70(8): 1294.

[2] Messler R W. Powder injection molding research at rensselaer: an update[J]. Metal Powder Report, 1989, 44(5): 362.

[3] Woodthorpe J, Edirisinghe M J, Evans J R G. Properties of ceramic injection moulding formulations (III) — polyner removal[J]. J Mater Sci, 1989, 24: 1038 - 1048.

[4] German R M. Theory of thermal debinding[J]. Int J Powder Metall, 1987, 72: 237 - 245.

[5] Cima M J, Dudziak M, Lewis J A. Observation of poly(vinyl butyral)-dibutyl phthalate binder capillary migration[J]. J Am Ceram Soc, 1989, 72: 1087.

[6] Cima M J, Lewis J A, Devoe A D. Binder distribution in ceramic greenware during thermolysis[J]. J Am Ceram Soc, 1989, 72(7): 1192 - 1199.

[7] Calvert P, Cima M. Theoretical models for binder burnout[J]. J Am Cer Soc, 1990, 73(3): 575 - 579.

[8] Lewis J A, Cima J A. Diffusion of dialkyl phthalates in plastized poly(vinly butyral)[J]. J Am Cer Soc, 1990, 73(9): 2702 - 2707.

[9] Mater S A, Edirisinghe M J, Evans J R G, et al. Modelling the removal of organic vehicle from ceramic or metal moulding: the effect of gas permeation on the incidence of defects[J]. J Mater Sci, 1995, 30: 3805 - 3810.

[10] German R M. Powder Injection Molding[M]. Princeton, NJ: Metal Powder Industries Federation, 1990. 321.

[11] Hwang K S, Tsou T H. Thermal debinding of powder injection molded parts: observations and mechanisms [J]. Metall Mater Trans A, 1992, 23A: 2775 - 2782.

[12] PIM 97. 1st European Sym. on PIM[J]. Powder Metallurgy, 1997, 40(4): 262 - 268.

[13] German R M, Hens K F. Identification of the Effects of Key Powder Characteristics on Powder Injection Molding[A]. Booker P, Gaspervich J, German R M. Powder Injection Molding Symposium —1992[C]. Princeton, NJ: Metal Powder Industries Federation, 1992, 1 - 15.

[14] Ohtsubo H, Maruta K, Nishimura K, et al. Deformation Behavior of Metal Injection Molded Compacts during Sintering[A]. Booker P, Gaspervich J, German R M. Powder Injection Molding Symposium —1992[C]. Princeton, NJ: Metal Powder Industries Federation, 1992, 393 - 407.

[15] LI Yi-min, HUANG Bo-yun, QU Xuan-hui. Rheology and debinding properties of wax-based thermal plastic binder in MIM[J]. Material Research Transaction, 1999, 13(6): 596 - 600. (in Chinese)

[16] Angermann H H, Van O O, Der Biest. Low temperature debinding kinetics of two-component model systems [J]. Inter J Powder Metall, 1993, 29(3): 239 - 250.

(Edited by LI Xiang-qun)